Design of Cross-talk Free Polarization Converter Based on Square-Lattice Elliptical-Hole Core Circular-Hole Holey Fibers

Design of Cross-talk Free Polarization Converter Based on Square Lattice Elliptical-Hole Core Circular-Hole Holey Fibers

ZEJUN ZHANG[1], YASUHIDE TSUJI[1,*], AND MASASHI EGUCHI[2]

[1] Division of Information and Electronic Engineering, Muroran Institute of Technology, Muroran, Japan, 050-8585
[2] Department of Photonics System Technology, Chitose Institute of Science and Technology, Chitose, Japan, 066-8655
[*] Corresponding author: y-tsuji@mmm.muroran-it.ac.jp

Compiled July 15, 2016

In this paper, a novel polarization converter (PC) based on square lattice elliptical-hole core circular-hole holey fibers (EC-CHFs) is proposed and analyzed. The proposed PC has oblique elliptical air holes in the core region, which can achieve polarization rotation with a conversion length as short as 31.7 μm. Additionally, in order to achieve a cross-talk free PC element, we propose a PC element with three cores which can completely convert polarization state by 90 degrees. The structural tolerance of the cross-talk free PC element has also been discussed in detail.

OCIS codes: *(060.2340) Fiber optics components; (130.5440) Polarization-selective devices.*

http://dx.doi.org/10.1364/ao.XX.XXXXXX

1. INTRODUCTION

In recent years, silicon-on-insulator (SOI) technology has been considered as a promising platform for photonic circuits due to the CMOS-compatible fabrication technology and the high refractive-index contrast of the waveguide structure [1, 2]. However, such high refractive indices also lead to a high polarization dependence of the group index [3]. In order to overcome this problem, a polarization diversity scheme could be employed. In this case, firstly, the orthogonal polarization components of incident light are split into two different waveguides by using a polarization splitter (PS). Then, the polarization of guided light in one of these waveguides is rotated 90° by using a polarization converter (PC). Therefore, in the rest of the photonic circuit, there is only one polarization has to be processed. In recent years, plenty of waveguide based PCs have been proposed [4–10], which can be classified into two major categories. One is based on the mode coupling, which utilizes the mode beating between two hybrid modes, such as PC waveguide with trench [5], or PC with an off-axis double-core structure [6], and so on. The other is based on the mode evolution, which is achieved by adiabatic mode transition, including PC with tapered or asymmetrical waveguide [7, 8], and some PCs with plasmon surface [9, 10]. Moreover, various polarization splitter-converters (PSCs) based on SOI waveguides have also been proposed so far [11–15]. In 2011, L. Liu *et al*. proposed a polarization splitting and rotating device built on the SOI platform with a total length of 36.8 μm [11]. The insertion loss is -0.6 dB and the extinction ratio is 12 dB. However, PSCs based on optical fibers have not been discussed popularly.

Photonic crystal fibers (PCFs) with a periodic array of air holes around the fiber core have been ardently studied recently owing to their unique lightwave guiding properties [16, 17]. PCs or PSs based on PCFs have also been studied [20–26]. In 2013, Hameed *et al*. proposed a passive ultra-compact polarization converter based on soft glass equiangular spiral photonic crystal fiber (ES-PCF) which offers 99% polarization conversion ratio with an ultra-compact device length of 96 μm [22]. However, the spiral structure complicates the fabrication process. Among the advantages of PCF, the single polarization transmission property is particularly attractive. A novel single-polarization holey fiber with a core consisting of elliptical holes, known as an elliptical-hole core circular-hole holey fiber (EC-CHF), has been proposed for achieving the absolutely single-polarization transmission easily [18, 19]. The EC-CHF can be designed to transmit only the x- or y-polarization easily by changing the major axis direction of the elliptical holes in the core region. In 2014, authors proposed a novel PS based on three triangular lattice EC-CHFs which can completely separate an arbitrarily polarized light beam into two orthogonal polarization states without any crosstalk with a device length of 630 μm [25, 26].

In this paper, we propose a novel PC element which has a symmetrical configuration based on EC-CHFs. Since the triangular lattice EC-CHF is difficult to realize the symmetrical configuration, here we adopt the EC-CHF with square lattice

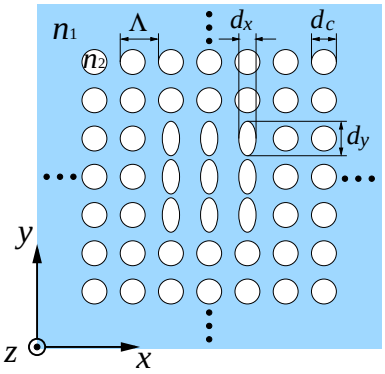

Fig. 1. Square lattice yEC-CHF with nine elliptical holes in the core region.

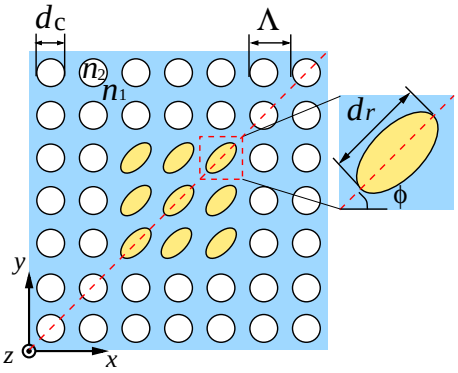

Fig. 2. Cross-section view of the single PC.

air holes, as shown in Fig. 1. In this paper, firstly, we propose a novel single PC element with oblique elliptical air holes in the core region, which can convert an x-polarized incident lightwave into a y-polarized wave. Then, in order to achieve cross-talk free property for a passive PC element, we adopt two EC-CHFs at both sides of the proposed PC as the input and output waveguides, respectively. Simulation results show that the PC with three cores can realize the completely polarization conversion and the extinction ratio (ER) of PC is infinitely high, *i.e.* the cross-talk free can be achieved. Here, we design the PC element using separated waveguides based on the coupled mode theory, this leads to a high design flexibility, such as a fiber type PSC would be achieved by combining our proposed three-core PC and the PS in [25, 26] based on square lattice EC-CHFs. In this paper, the full-vectorial finite element method (FV-FEM) [27] has been used to estimate the modal effective index of waveguide, and the propagation of incident light has been analyzed by using the full-vector finite element beam propagation method (FE-BPM) [28].

2. STRUCTURE OF PC

The cross-sectional structure of a square lattice EC-CHF is shown in Fig. 1. All the air-holes are arranged in a square pattern and the core region consists of nine elliptical holes whose major axis is aligned along the y-direction. This kind of EC-CHF can transmit only y-polarized waves, and it is referred to as a yEC-CHF [25]. Due to the symmetry property of square pattern, if we rotate a yEC-CHF by 90 degrees, an xEC-CHF with the major axis of ellipses along the x-direction can be obtained to transmit only x-polarized waves.

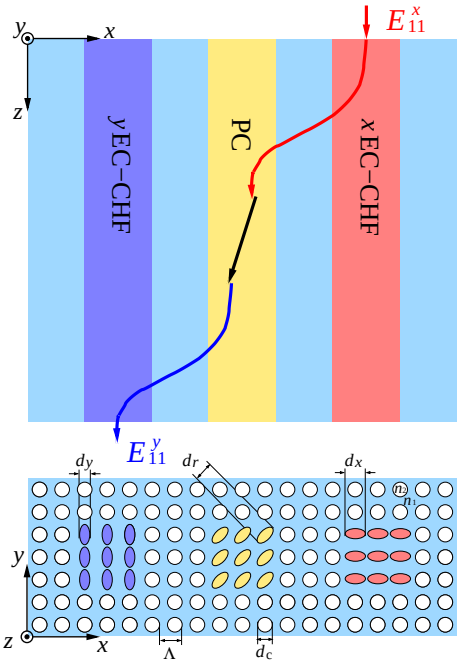

Fig. 3. Schematic and cross-sectional view of our proposed PC element based on three-core EC-CHFs.

In this paper, we propose a novel single passive PC element based on a square lattice EC-CHF, which has nine oblique elliptical holes in the core region ($\phi = 45°$), as shown in Fig. 2. The incident orthogonal polarized component can be converted by 90 degrees. However, since both of x- and y-polarization exist in the PC, then the ER of the single PC element should be considered. In order to achieve the cross-talk free property, we adopt two EC-CHFs at both sides of the PC waveguide, whose schematic and cross-sectional view are illustrated in Fig. 3. We use two EC-CHFs as the input and output waveguides of the PC element to ensure the single-polarized output wave. As shown in Fig. 3, if a beam of x-polarized light wave is launched into the xEC-CHF at right side, since the adjacent two waveguides (the xEC-CHF and the PC waveguide) are close enough, the x-polarized incident light would be coupled into the PC waveguide and converted by 90 degrees, *i.e.* the y-polarized component. In the same way, the generated y-polarized component would be coupled into the yEC-CHF at left side due to the single-polarization property of EC-CHF. Therefore, for the output waveguide, there is only the y-polarized component, and the cross-talk free property can be achieved. Additionally, if a beam of y-polarized light wave is launched into the left yEC-CHF, then only the converted x-polarized component is output from the xEC-CHF at right side.

The basic structural parameters are set as follows: the hole pitch Λ is 1 μm, all the elliptical-holes have the same ellipticity of $d_{\text{major}}/d_{\text{minor}} = 2$, the refractive indices of silica and air holes are $n_1 = 1.45$ and $n_2 = 1$, respectively, and the operation wavelength is set to $\lambda = 1.55$ μm. In order to design a PC element, the guided modes in coupled and isolated systems are analyzed by using the FV-FEM, and the light propagation in the PC is simulated by using the FE-BPM.

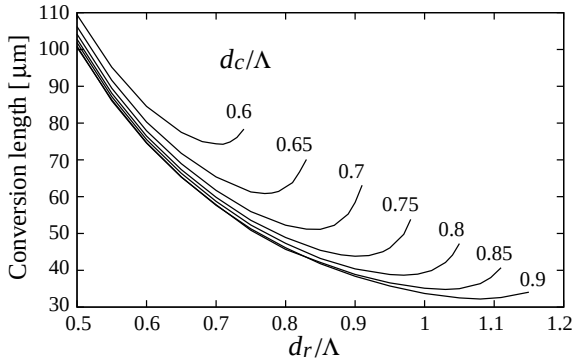

Fig. 4. Hole size dependence of the conversion length ($\lambda = 1.55\ \mu$m).

Table 1. Minimum conversion length and its corresponding elliptical-hole size for different hole sizes in the cladding

d_c/Λ	d_r/Λ	Min. of L_r [μm]
0.60	0.71	74.25
0.65	0.77	60.85
0.70	0.85	51.13
0.75	0.90	43.84
0.80	0.97	38.69
0.85	1.03	34.80
0.90	1.08	32.20
0.91	1.09	31.70

3. DESIGN OF PC ELEMENT WITH SQUARE LATTICE EC-CHFS

A. Design of Single PC Element

In this subsection, we will introduce the design of a single PC based on a square lattice EC-CHF. The cross-sectional view of our proposed single PC is illustrated in Fig. 2. The PC waveguide has nine oblique elliptical holes in the core region whose major axis is rotated counter clockwise by $\phi = 45°$ with respect to the x-axis. Since the structure has symmetry with respect to $y = x$, incident x- or y-polarized waves can be completely rotated 90°. Refer to [21], the hybridness is defined as

$$\text{Hybridness} = \max\left|H_\mu\right| / \max\left|H_\nu\right| \quad \textbf{(1)}$$

where μ and ν are x and y for x-polarized mode while y and x for y-polarized mode, respectively. The conversion length L_r is defined as $L_r = 0.5\lambda/(n_{\text{eff},1} - n_{\text{eff},2})$, where λ is the operating wavelength, $n_{\text{eff},1}$ and $n_{\text{eff},2}$ represent the effective indices of two eigenmodes of the single PC. With the elliptical holes in the core, the PC element has a large birefringence which leads to a short conversion length.

The hole size dependence of conversion length has been investigated in detail, as shown in Fig. 4. We note that with a constant hole size in the cladding, the conversion length decreases when d_r increases at first, and then it has a slight increase after reaching the minimum value. This is because the larger elliptical holes make birefringence larger. However, with the elliptical-hole size getting larger, most of the light spreads into the birefringence-free cladding region, and this leads to a longer conversion length. Moreover, it also can be observed that the minimum value of conversion length decreases with larger circular-holes in the cladding. Table 1 shows the minimum conversion length, and its corresponding major axis length of elliptical hole in the core and hole size in the cladding. The shortest conversion length that we have obtained is $L_r = 31.7\ \mu$m with hole sizes of $d_c = 0.91\Lambda$ and $d_r = 1.09\Lambda$. Figure 5 shows the magnetic field distributions of H_x and H_y components for the fundamental and 1^{st}-higher-order modes, respectively. It can be observed that the two field profiles are very similar, and the hybridness is 0.99994 for the fundamental mode and 0.99921 for the 1^{st}-higher-order mode. The propagation behaviors obtained by the FE-BPM with the shortest conversion length are shown in Fig. 6. It can be observed that an x-polarized incident light can be completely converted into a y-polarized light through our proposed PC. However, since both of the x- and y-polarized components exist in the same waveguide, the ER for this PC element should be estimated. Here, the ER is defined as

$$\text{ER} = 10\log_{10}\frac{\text{Output power of } x\text{-polarization}}{\text{Output power of } y\text{-polarization}}. \quad \textbf{(2)}$$

A BPM simulation shows that the ER is -23dB at $\lambda = 1.55\mu$m. Here, the longitudinal step size is set to 1 μm, the analyzed region of $13 \times 13\ \mu$m is discretized using curvilinear hybrid edge/nodal elements [27]. An adaptive mesh [28] is used and the total unknowns are 191,559.

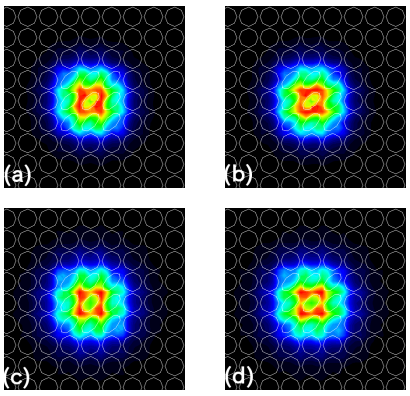

Fig. 5. Magnetic field distributions of the (a) H_x and (b) H_y components for the fundamental mode, and the (c) H_x and (d) H_y components for the 1^{st}-higher-order mode.

B. Design of Cross-talk Free Three-core PC Element

In the previous subsection, we designed a single PC element based on a square lattice EC-CHF. In general, considering the deviation of hole sizes in the fabrication process, 100% conversion is difficult to achieve and a considerable ER may exist in this PC. However, in our study, in order to realize the cross-talk free device, a yEC-CHF and an xEC-CHF are added at both sides of the PC waveguide presented in the previous subsection to ensure that the input and output waves are absolutely single-polarized. Fig. 3 shows the cross-sectional structure of our proposed cross-talk free three-core fiber PC element. Here we set the PC waveguide in the middle, and design the hole size of PC waveguide by satisfying the phase matching condition with two EC-CHFs. According to the coupled mode theory, if an x-polarized light beam is launched into the xEC-CHF, it would

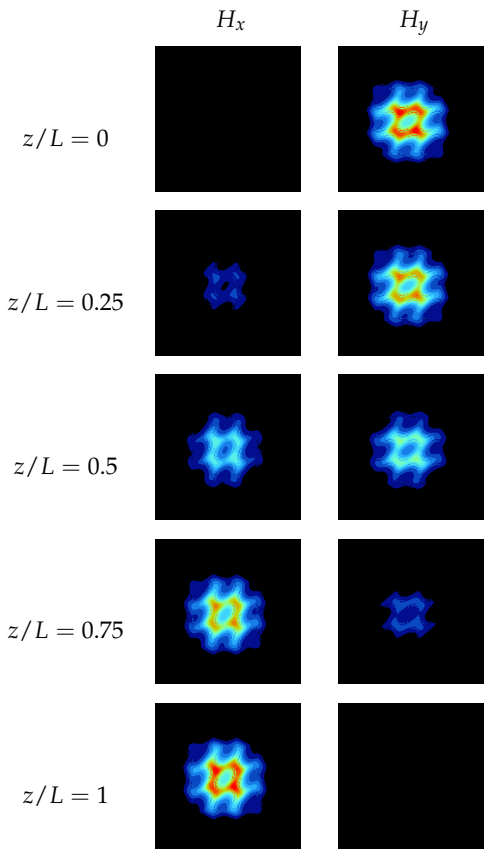

Fig. 6. Propagation behavior in the PC ($L_r = 31.7\ \mu$m).

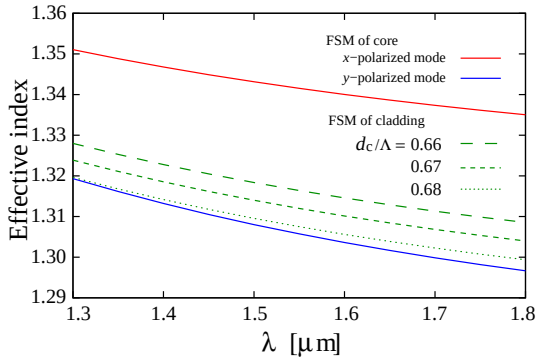

Fig. 7. Dispersion curves of the xEC-CHF.

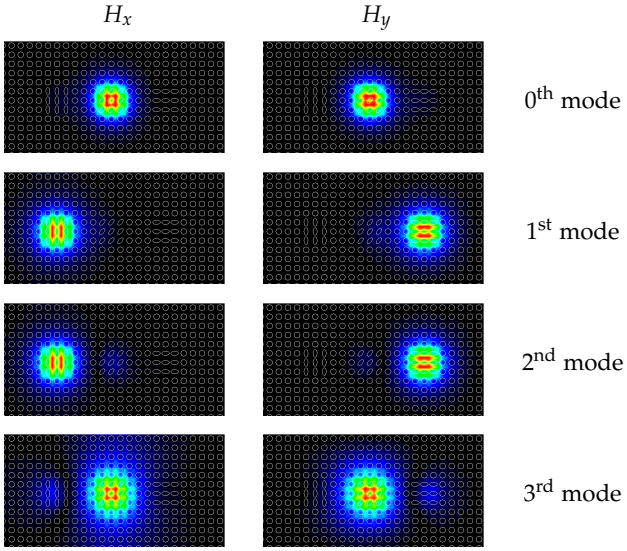

Fig. 8. Modal field distribution of each coupled mode with $d_r/\Lambda = 0.835$.

be coupled into the PC and converted into a y-polarized light; then the converted y-polarized component would be coupled into the yEC-CHF at the left side. Owing to the square lattice arrangement, the yEC-CHF and xEC-CHF have the same hole sizes for satisfying the phase matching condition. Therefore, we set the xEC-CHF at right side as the reference waveguide, the major axis length of elliptical-holes is set to $d_x = 0.9\Lambda$. The dispersion curves of the xEC-CHF are illustrated in Fig. 7, we note that the EC-CHF has a large birefringence by introducing elliptical holes in the core, the effective index of fundamental space-filling mode (FSM) for the x-polarization is much higher than the y-polarization. Three dashed curves between the FSMs of x- and y-polarizations represent the FSM of cladding with different circular hole sizes, *i.e.* $d_c/\Lambda = 0.66$, 0.67 and 0.68. In order to achieve the single-polarization with a wide bandwidth for the EC-CHF, the hole size in the cladding is set to $d_c/\Lambda = 0.66$. The effective index of the xEC-CHF in an isolated system is $n_{\text{eff},x} = 1.32531$.

Then, we design the phase matching hole size in the core of PC waveguide. Since the PC waveguide has two eigenmodes, here we determine d_r by meeting $n_{\text{eff,pc}} = n_{\text{eff},x}$, where $n_{\text{eff,pc}}$ is the average value of effective indices of the two eigenmodes, and the corresponding d_r is $d_r/\Lambda = 0.835$.

In the coupled system, for the PC element with the determined parameters, we note that four kinds of coupled modes exist (*i.e.*, both x- and y-polarized modes in the PC, the single x- and y-polarized modes in the xEC-CHF and yEC-CHF, respectively, are coupled to each other.) and the polarization conversion is achieved by utilizing these mode couplings. The modal field distribution of each coupled mode with $d_r/\Lambda = 0.835$ is illustrated in Fig. 8. It can be observed that the four coupled modes are almost isolated. In this case, the polarization conversion is achieved through the coupling between the 1st- and 2nd-modes. The polarization conversion with these modes requires a relatively long conversion length since the coupling length depends on the minimum index difference between these coupled modes. In order to obtain a short conversion length and ensure the single-polarization state of the EC-CHFs, we investigate the variation of four coupled modes against d_r, as shown in Fig. 9. Based on the coupled mode theory for three coupled modes, the same effective index difference between the coupled modes is required to achieve a short conversion length. Therefore, we investigate the variation of four coupled modes near $d_r/\Lambda = 0.795$ and 0.865 in detail, as shown in Figs. 10 (a) and (b), respectively. The figures show that the refractive indices of three coupled modes in the bottom have the same index difference $\Delta = 5 \times 10^{-4}$ at $d_r/\Lambda = 0.798$. In addition, the same index difference $\Delta = 5 \times 10^{-4}$ can also be obtained at $d_r/\Lambda = 0.867$. Here, we use $d_r/\Lambda = 0.798$ to design the PC. The modal field distribution of each coupled mode is illustrated in Fig. 11. The first coupled modes of H_x and H_y are almost isolated and do not contribute to the polarization conversion, while the other

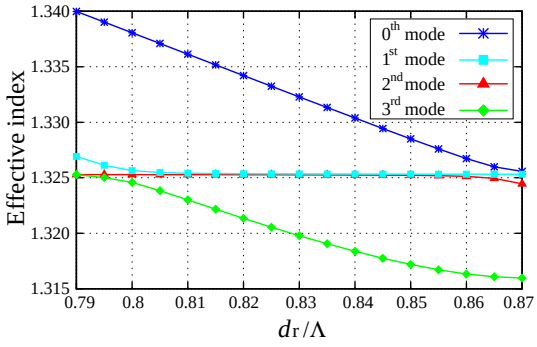

Fig. 9. Effective indices of four coupled modes against d_r.

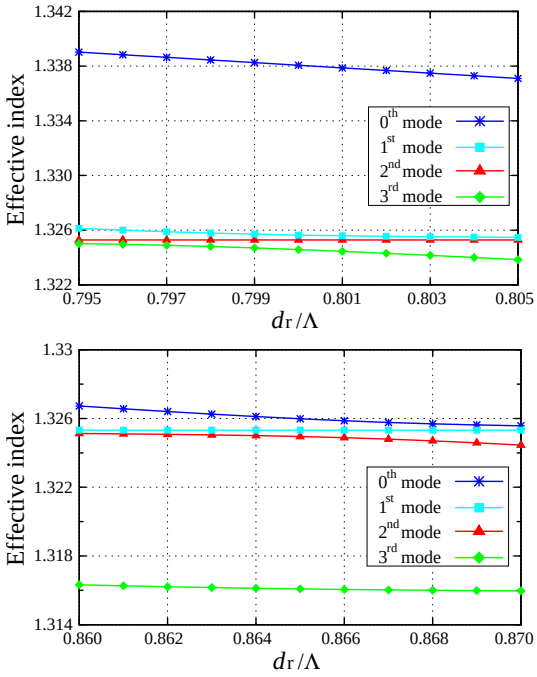

Fig. 10. Effective indices of four coupled modes against d_r (a) near $d_r/\Lambda = 0.795$, (b) near $d_r/\Lambda = 0.865$.

three coupled modes contribute to the polarization conversion.

The propagation behaviors in the PC with a conversion length of $L_r = 1550$ μm are simulated by using the FE-BPM, as shown in Fig. 12. Here, the longitudinal step size is set to 1 μm, the analyzed region is 25×13 μm, and the total unknowns are 429,251. We can observe that after an x-polarized light is launched into the xEC-CHF, it is completely converted into a y-polarized light through our proposed PC. The ER of three-core PC element can be illustrated as follows,

$$\mathrm{ER} = 10\log_{10}\frac{P_{1y\to 3x} + P_{1y\to 3y} + P_{1x\to 3x}}{P_{1x\to 3y}}. \quad (3)$$

where P_{1x} and P_{1y} respect to the power of x- and y-polarizations in the input waveguide xEC-CHF, P_{3x} and P_{3y} are the power of x- and y-polarizations in the output waveguide yEC-CHF, $P_{1y\to 3x}$ and $P_{1x\to 3x}$ represent the x-polarization in output waveguide which is converted by the P_{1y} and P_{1x}, respectively. In the same way, $P_{1y\to 3y}$ and $P_{1x\to 3y}$ represent the y-polarization in output waveguide which is converted by the P_{1y} and P_{1x}, respectively. Owning to the absolutely single-

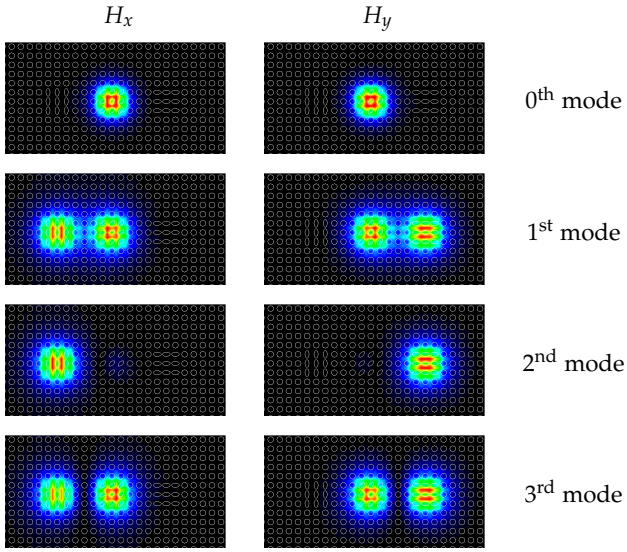

Fig. 11. Modal field distribution of each coupled mode with $d_r/\Lambda = 0.798$.

polarization property of an EC-CHF, P_{1y} for the xEC-CHF is 0, and P_{3x} for the yEC-CHF is 0. Therefore, the numerator of the ER fraction is 0, and the ER is infinitely high, the cross-talk free property is achieved.

C. Structure tolerance of PC element with three-core EC-CHF

So far, we have proposed and designed a novel PC element based on three-core EC-CHFs. Considering the current fabrication technology of PCF, one of the difficulties in our proposed PC element is the deviation of the air holes away from the designed values. Here, we wish to further discuss the structural tolerance of the three-core PC element. Since two EC-CHFs on both sides are the key components to obtain the cross-talk free property, firstly, we investigate the absolutely single-polarization of the xEC-CHF with various geometric elliptical holes. In our designing process, the major axis of elliptical hole is $d_x/\Lambda = 0.9$, and the ellipticity is $d_{\mathrm{major}}/d_{\mathrm{minor}} = 2$. However, in practical manufacturing process, the ellipticity is difficult to maintain in 2, thus we investigate the xEC-CHF dispersion curves against a variation d_x while the elliptical hole area is unchanged, as shown in Fig. 13. The green dashed line represents the constant FSM in the cladding ($d_c/\Lambda = 0.66$). It can be observed that the elliptical holes in the core with a large d_x lead to a large birefringence, and the single polarization can be easily achieved. While due to $d_x < \Lambda$, we only take into account the d_x increased by 9%. In addition, if the major axis d_x decreases 15% ($d_x/\Lambda = 0.765$), the FSM of y-polarization of core is almost the same as the FSM in the cladding. Therefore, in our research, the single-polarization property of the xEC-CHF can be achieved with $d_x/\Lambda > 0.765$ by keeping the hole area.

After we discussed the structure tolerance of the single-polarized EC-CHF, we will focus on the inclination angle of the elliptical holes in PC waveguide. As we demonstrated in the last subsection, the PC waveguide whose elliptical hole inclination angle is $\phi = 45°$ can convert an x-polarized incident light by 90 degree with a low ER. If the inclination angle fluctuates, the symmetrical structure of the PC will be destroyed, and the completely polarization conversion will be difficult to achieve. For the three-core PC element, the cross-talk free prop-

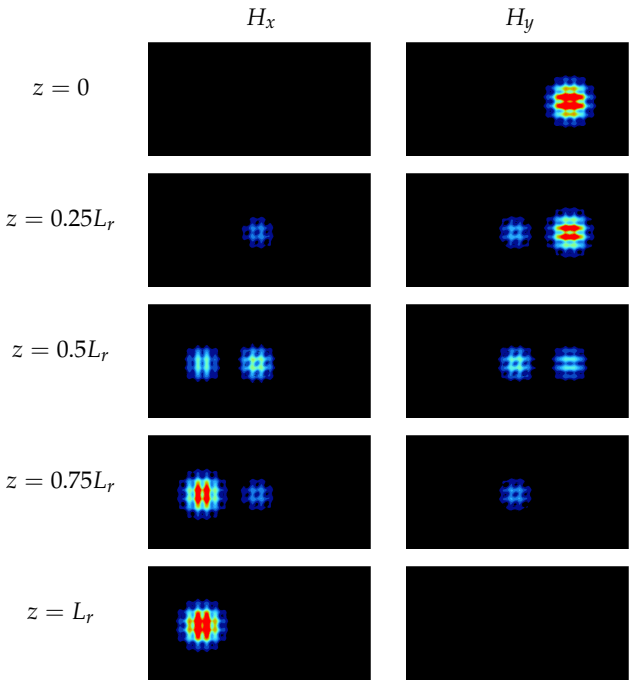

Fig. 12. Propagation behavior in three-core PC element (L_r = 1550 μm).

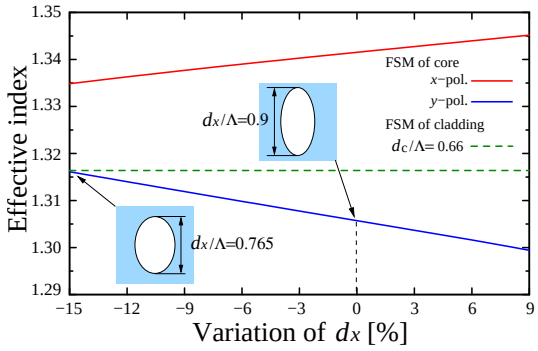

Fig. 13. Effective index variation of the xEC-CHF against the major axis d_x by keeing the elliptical hole area (λ = 1.55 μm).

erty still can be achieved since the EC-CHF is used as output waveguide, while the inclination angle fluctuation leads to a low conversion efficiency. Based on the three-core PC parameters designed before, the major axis length of elliptical holes in EC-CHF is $d_x/\Lambda = 0.9$, $d_r/\Lambda = 0.798$ for the PC waveguide in the middle, $d_c/\Lambda = 0.66$ for the cladding holes, the ellipticity is set to 2, each core is separated from the adjacent cores by three air holes, and the device length is fixed to 1550 μm. The conversion efficiency is calculated by

$$\eta = \frac{P_{3y}}{P_{1x}} \times 100\%. \quad \textbf{(4)}$$

where P_{3y} is the power of converted y-polarization in the output waveguide yEC-CHF and P_{1x} is the power of incident x-polarization in the input waveguide xEC-CHF. The variation of conversion efficiency against the fluctuated inclination angle is illustrated in Fig. 14. It can be observed that the conversion efficiency is better than 90% when the inclination angle is set

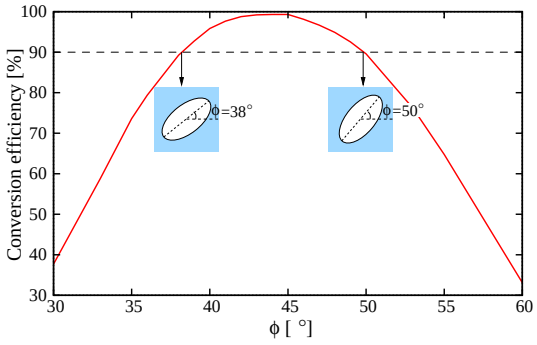

Fig. 14. Conversion efficiency of the three-core PC element against the inclination angle of elliptical holes in the PC waveguide.

Fig. 15. Conversion efficiency versus the deviation for different parts of the device parameters at each deviation level

Deviation	Core region			Cladding
level	xEC-CHF	PC	yEC-CHF	region
-0.2%	87.4%	77.3%	87.6%	98.2%
-0.1%	95.7%	92.1%	95.8%	98.3%
0	99.1%	99.1%	99.1%	99.1%
0.1%	95.0%	94.1%	94.8%	98.3%
0.2%	86.1%	81.6%	85.9%	98.1%

between 38° ∼ 50°.

Finally, we examined the conversion efficiency versus the deviation for the respective hole sizes of each region, as shown in Table 15. Here, all the hole sizes of the deviation part are varied with the same extent, such as if only the holes in xEC-CHF core region are expanded 0.1%, the coupling efficiency of the PC will decrease to 95% because the phase matching condition is mismatched between the xEC-CHF and PC waveguide. In the practical manufacturing process, all the hole sizes vary randomly, however, the deviation for one part of the device with the same extent leads to a worse conversion efficiency. Here, we investigate the worse conversion efficiency, while a better conversion efficiency can be obtained in the fabrication process. It can be observed that the conversion efficiency with the deviation of elliptical holes is much worse than the varies in the cladding. That is because in an EC-CHF the effective index is sensitive to the hole sizes in the core region. So if we design this type of PC using a single-polarized PCF with only circular air holes, such as the PCF in [29], it may be possible to obtain a device with larger tolerance. Moreover, in the design of three-core PC element, in order to obtain the clear magnetic distributions of coupled modes, we adopt three column air holes between the adjacent cores. Since the large core interval leads to a low structural tolerance, if the mode coupling part of this PC is scaled down using a tapered structure [30], the narrow core interval will increase the tolerance.

4. CONCLUSION

In this paper, we proposed a novel passive PC element based on square lattice EC-CHFs. The single PC element can achieve

the polarization conversion with a short conversion length of 31.7 μm, and the ER is better than -23dB. In order to realize a cross-talk free structure, we have also designed a three-core PC element which has two single-polarized EC-CHFs at both sides of the PC waveguide. The simulation results demonstrated that when an x-polarized incident light beam is launched into the input waveguide xEC-CHF, it is completely rotated to a y-polarized component and coupled into the output waveguide yEC-CHF. The total device length is 1550 μm. Moreover, considering the practical application and the current fabrication technology of PCF, the structural tolerances of three-core PC element have been discussed in detail, including the single-polarization property of EC-CHF, the inclination angle fluctuation in PC waveguide, and the deviation of air holes. In order to realize the PC with a large tolerance, using PCF with only circular air holes and adopting the tapered structure for the mode coupling part are the focuses of our future work.

REFERENCES

1. T. Tsuchizawa, K. Yamada, H. Fukuda, T. Watanabe, J. Takahashi, M. Takahashi, T. Shoji, E. Tamechika, S. Itabashi, and H. Morita, "Microphotonics devices based on silicon microfabrication technology," IEEE J. Sel. Topics Quantum Electron. **11**, 232–240 (2005).
2. W. Bogaerts, R. Baets, P. Dumon, V. Wiaux, S. Beckx, D. Taillaert, B. Luyssaert, J. Van Campenhout, P. Bienstman, and D. Van Thourhout, "Nanophotonic waveguides in silicon-on-insulator fabricated with CMOS technology," J. Ligthw. Technol. **23**, 401–402 (2005).
3. E. Dulkeith, F. Xia, L. Schares, W. M. J. Green, and Y. A. Vlasov, "Group index and group velocity dispersion in silicon-on-insulator photonic wires," Opt. Express **14**, 3853–3863 (2006).
4. D. C. Hutchings and B. M. Holmes, "A waveguide polarization toolset design based on mode beating," IEEE Photon. J. **3**, 450–461 (2011).
5. S.-H. Kim, R. Takei, Y. Shoji, and T. Mizumoto, "Single-trench waveguide TE-TM mode converter," Opt. Express **17**, 11267–11273 (2009).
6. H. Fukuda, K. Yamada, T. Tsuchizawa, T. Watanabe, H. Shinojima, and S. Itabashi, "Polarization rotator based on silicon wire waveguides," Opt. Express **16**, 2628–2635 (2008).
7. J. Zhang, M. Yu, G.-Q. Lo, and D. L. Kwong, "Silicon-waveguide based mode evolution polarization rotator," IEEE J. Quantum Electron. **16**, 53–60 (2010).
8. W. Xu, W. Ye, X. Yuan, Z. Zhu, and Q. Lu, "Proposal for ultra-compact silicon-on-insulator waveguide polarization converter," IEEE Photon. Technol. Lett. **26**, 447–450 (2014).
9. J. Zhang, S. Y. Zhu, H. J. Zhang, S. Y. Chen, G.-Q. Lo, and D. L. Kwong, "An ultra-compact surface plasmon polariton-effect-based polarization rotator," IEEE Photon. Technol. Lett. **23**, 1606–1608 (2011).
10. J. N. Caspers, M. Z. Alam, and M. Mojahedi, "Compact hybrid plasmonic polarization rotator," Opt. Lett. **37**, 4615–4617 (2012).
11. L. Liu, Y. Ding, K. Yvind, and J. M. Hvam, "Silicon-on-insulator polarization splitting and rotating device for polarization diversity circuits," Opt. Express **19**, 12646–12651 (2011).
12. D. Dai, and J. E. Bowers, "Novel concept for ultracompact polarization splitter-rotator based on silicon nanowires," Opt. Express **19**, 10940–10949 (2011).
13. Y. Ding, L. Liu, C. Peucheret, and H. Ou, "Fabrication tolerant polarization splitter and rotator based on a tapered directional coupler," Opt. Express **20**, 20022–20028 (2012).
14. H. Guan, A. Novack, M. Streshinsky, R. Shi, Q. Fang, A. E. Lim, G. Lo, T. B. Jones, and M. Hochberg, "CMOS-compatible highly efficient polarization splitter and rotator based on a double-etched directional coupler," Opt. Express **22**, 2489–2496 (2014).
15. W. D. Sacher, T. Barwicz, B. J. F. Taylor, and J. K. S. Poon, "Polarization rotator-splitters in standard active silicon photonics platforms," Opt. Express **22**, 3777-3786 (2014).
16. J. C. Knight, T. A. Birks, P. St. J. Russell, and D. M. Atkin, "All-silica single-mode optical fiber with photonic crystal cladding," Opt. Lett. **21**, 1547–1549 (1996).
17. P. St. J. Russell, "Photonic-crystal fibers," J. Ligthw. Technol. **24**, 4729–4749 (2006).
18. M. Eguchi and Y. Tsuji, "Single-mode single-polarization holey fiber using anisotropic fundamental space-filling mode," Opt. Lett. **32**, 2112–2114 (2007).
19. M. Eguchi and Y. Tsuji, "Design of single-polarization elliptical-hole core circular-hole holey fibers with zero dispersion at 1.55 μm," J. Opt. Soc. Amer. B **25**, 1690–1701 (2008).
20. M. F. O. Hameed, S. S. A. Obayya, and H. A. El-Mikati, "Passive polarization converters based on photonic crystal fiber with L-shaped core region," J. Ligthw. Technol. **30**, 283–289 (2011).
21. M. F. O. Hameed, and S. S. A. Obayya, "Polarization rotator based on soft glass photonic crystal fiber with liquid crystal core," J. Ligthw. Technol. **29**, 2725–2731 (2011).
22. M. F. O. Hameed, A. M. Heikal, and S. S. A. Obayya, "Novel passive polarization rotator based on spiral photonic crystal fiber," IEEE Photon. Technol. Lett. **25**, 1578–1581 (2013).
23. M. Chen, B. Sun, Y. Zhang and X. Fu, "Design of broadband polarization splitter based on partial coupling in square-lattice phtotnic-crystal fiber," Appl. Opt. **49**, 3042–3048 (2010).
24. W. Lu, S. Lou, X. Wang, L. Wang and R. Feng, "Ultrabroadband polarization splitter based on three-core photonic crystal fibers," Appl. Opt. **52**, 449–455 (2013).
25. Z. Zhang, Y. Tsuji and M. Eguchi, "Design of polarization splitter with single-polarized elliptical-hole core circular-hole holey fibers," IEEE Photon. Technol. Lett. **26**, 541–543 (2014).
26. Z. Zhang, Y. Tsuji and M. Eguchi, "Study on crosstalk-free polarization splitter with elliptical-hole core circular-hole holey fibers," J. Ligthw. Technol. **32**, 3956–3962 (2014).
27. M. Koshiba and Y. Tsuji, "Curvilinear hybrid edge/nodal elements with triangular shape for guidedwave problems," J. Ligthw. Technol **18**, 737–743 (2000).
28. Y. Tsuji and M. Koshiba, "Adaptive mesh generation for full-vectorial guided-mode and beam propagation solutions," J. Sel. Topics Quantum Electron. **6**, 163–169 (2000).
29. K. Ichikawa, Z. Zhang, Y. Tsuji, and M. Eguchi, "single-polarization holey fiber with anisotropic lattice of circular air holes," J. Ligthw. Technol. **33**, 3866–3871 (2015).
30. E. C. M$\ddot{a}$gi, P. Steinvurzel, and B. J. Eggleton, "Tapered photonic crystal fibers," Opt. Express **12**, 776–784 (2004).